EFFECT OF AGING ON MECHANICAL PROPERTIES OF 316LN AT 4.2 K FOR FUSION APPLICATIONS

Jan Sas[1)], Sandra Kauffmann-Weiss[1)], Klaus-Peter Weiss[1)]*
[1)] *Karlsruhe Institute of Technology, Institute for Technical Physics, Eggenstein-Leopoldshafen, Germany*

Received: 30.07.2018
Accepted: 03.12.2018

[*]*Corresponding author: e-mail: jan.sas@kit.edu, Tel.: +49 721 608 24164, Karlsruhe Institute of Technology, Institute for Technical Physics, Hermann-von-Helmholtz-Platz 1, 763 44 Eggenstein-Leopoldshafen, Germany*

Abstract
Within the fusion magnet technology the low-temperature superconductor Nb_3Sn is usually used for high magnetic field in the range of 12 T and 4.5 K. These superconductors are produced as round strands. Here Nb_3Sn filaments are embedded in a round copper matrix with a diameter of about 0.8 mm. To allow magnet windings of several Mega-Ampere to produce the needed magnetic field, about 900 superconducting strands are cabled and compacted in a stainless steel conduit resembling the so-called cable-in-conduit-conductor (CICC). However, the mechanically brittle Nb_3Sn superconducting phase is produced by the diffusion reaction by a long-term heat treatment. Therefore, the magnet winding containing the superconducting strands together with the stainless steel jacket has to undergo this heat treatment. In order to simulate the magnet manufacturing process, seamless tubes were compacted, bend and straightened and tensile stretched by 2.5 % at room temperature followed by the heat treatment necessary for the Nb_3Sn formation. The aim of this study was to compare the microstructures and tensile properties at cryogenic operation temperature of two modified 316LN austenitic stainless steels with very-low carbon ($\leq$ 0.013) in the as built conditions and after heat treatments. Scanning Electron Microscopy (SEM), Electron Backscatter Diffraction (EBSD) and X-ray diffraction were used to study microstructure. Deformation behaviour was investigated by tensile test at 4.2 K.

Keywords: 316LN, Mechanical properties, Cryogenic temperature, Fusion magnets

1 Introduction

Large-scale superconducting magnets are often built applying the cable in conduit conductor (CICC) technology [1]. Depending on the necessary electrical current of such superconducting cables and the magnetic field at the conductor, this technology implements the possibility to optimize the inductance and a force flow cooling with Helium to a temperature of about 4.5 K. Especially for the plasma confinement within fusion research, several design concepts exists and are in operation. For magnetic fields lower than 10 T NbTi alloys are typically used as superconductors, e.g. in the Large Helical Device (LHD) [2], in Wendelstein-7X [3] and in the newly built Japan Torus JT60-SA [4]. Going to even higher magnetic fields above 11 T Nb_3Sn has to be used. Presently, the largest magnetic confinement experiment under construction using this alloy is ITER [5]. Since Nb_3Sn is a brittle intermetallic phase, several process routes exist to

DOI 10.12776/ams.v24i4.1140 p-ISSN 1335-1532
e-ISSN 1338-1156

manufacture wires that can be further used for cabling of these superconducting strands and jacketing of the cable [6] into a stainless steel tube or conduit to build the CICC. All of them have in common that Nb and Sn are separate during the manufacturing process and are diffusion-reacted by an additional heat treatment to finally form the superconducting phase Nb_3Sn. However, this technology demands that the conduit is also subjected to this reaction annealing process, as the conduit is part of the superconducting CICC.

A typical structural conduit material used for these CICC operating at cryogenic temperatures down to 4.2 K is the austenitic stainless steel 316LN [7]. Especially the high-nitrogen austenitic steel, 316LN was qualified for that temperature by numerous experiments in the past [8-15]. 316LN has a wide application for cryogenic components and an excellent combination of mechanical and physical properties such as resistance to neutron radiation and corrosion [7]. However, heat treatments can generally promote the formation of carbides and nitrides. Up to 18 different precipitations were observed [16] and appear intergranular and transgranular [17]. In high-nitrogen, austenitic steel an increased nitrogen level is used in order to stabilize the austenite while nickel is reduced. Intergranular Cr_2N precipitates can form easily, which affects the mechanical properties and the corrosion behaviour [6]. Thus, it is necessary to investigate the effect of cold working (during jacketing of the cable) and annealing on the nitride and carbide formation in high-nitrogen austenitic stainless steels.

In the present article, two compositions of high-nitrogen austenitic stainless steel, developed for applications as conduit materials in superconducting CICC were exemplarily investigated. We examine the influence of cold working and long-term aging microstructure and mechanical properties at 4.2 K of 316LN stainless steel. Annealing temperatures between 600 °C (about 870 K) and 650 °C (about 920 K) and long aging duration of up to 432 h were applied in order to cover the microstructural evolution similar to that occurring during processing of Nb_3Sn conduit conductors.

2 Experiments

In order to reproduce the magnet manufacturing process, the seamless tubes with an original outer diameter of 48 mm were compacted, bend and straightened followed by a tensile stretching by 2.5 % at room temperature to a final jacket with 43.5 mm outer diameter and 2 mm wall thickness. After this deformation aging in argon atmosphere was performed. One series was annealed at 866 K for 130 h and 890 K for 300 h (HT1) and second series at 920 K for 200 h (HT2), which represents different CICC preparation methods [6, 18]. Tensile tests were performed at 4.2 K on sub-size specimens which were cut by electrical discharge machining with a width of 12.5 mm and a thickness of 2 mm (ASTM E8M standard), with a displacement rate of 0.5 mm/min and a gauge length of 50 mm using a universal servo-hydraulic testing machine [19] equipped with a cryostat system. The cryostat with a vacuum shield was used for the cool down process to liquid helium temperature. Every test series consists of at least three specimens with tensile direction along the tube axis.

X-ray diffraction (XRD) experiments were carried out on a Bruker D8 diffractometer in Bragg-Brentano geometry. The Cu X-ray tube was operated at 40 kV and 40 mA. For these measurements a motorized slit of 0.7 mm and a 2.5° axial Soller slit were used at the source as well as two motorized slits of 9 mm, a 2.5° axial Soller slit and a Ni filter at the Lynxeye-XE 1D-detector. The diffraction pattern was determined between 20° and 120° with steps of 0.01° for 1 s each. For the chemical analyses, optical emission spectrometry using a Bruker Q4

DOI 10.12776/ams.v24i4.1140 p-ISSN 1335-1532
e-ISSN 1338-1156

Tasman and inert gas fusion analysis (nitrogen content) using a Bruker G8 Galileo were utilised. Cross sections were prepared by standard metallographic procedure including grinding up to a grid of P4000 and subsequent polishing with 1 µm diamond suspension as well as oxide polishing suspension OP-S and finally vibratory polishing. For microstructure investigations, backscatter electron imaging (BSE) and orientation imaging microscopy by electron backscatter diffraction (EBSD) were performed using a Zeiss LEO 1530 scanning electron microscope (SEM). The EBSD orientation maps were obtained by indexing a 650 x 500 pixel area with step size of 1 µm while the SEM was operated at 20 kV (with 90 µm aperture).

3 Results and Discussion

3.1 Mechanical properties

In this study, we investigated two modified alloys based on 316LN austenitic stainless steels. The according chemical compositions are presented in **Table 1**. Both materials exhibit a carbon content lower than 0.013 wt.%. Thus, in contrast to 316LN according to European standard (EN 10028-7) which contains 0.03 wt.% C, the carbon content is significantly reduced. Furthermore, the nitrogen content of Mat-1 is 0.174 wt.% and close to the maximum 0.22 wt.% standardized in EN 10028-7. Mat-2 has lower nitrogen content of 0.131 wt.% and is thus closer to the minimum value of 0.12 wt.%.

Table 1 Chemical composition of the two different modified 316LN austenitic stainless steels, all in wt.%

	C	Si	Mn	Cr	Ni	P	S	N	Mo
Mat-1	0.013	0.152	1.668	17.25	13.71	0.019	< 0.005	0.174	2.537
Mat-2	0.011	0.332	1.79	17.36	13.58	0.006	< 0.005	0.131	2.671

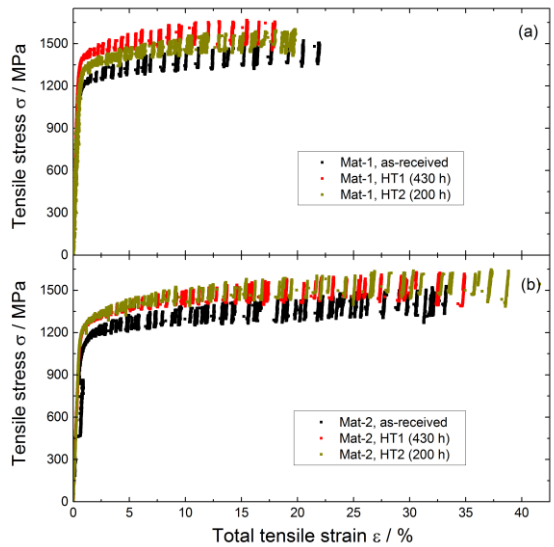

Fig. 1 Stress-strain dependence of selected tensile tests until fracture at 4.2 K

In order to simulate the magnet manufacturing process, seamless tubes from both materials are as described in section 2 compacted, bend and straightened followed by a tensile stretching by

DOI 10.12776/ams.v24i4.1140 p-ISSN 1335-1532
e-ISSN 1338-1156

2.5 % at room temperature. The mechanical deformation process is followed by a heat treatment. Tensile specimen are cut for further characterization.

Fig. 1 shows the engineering stress strain curves at the operating temperature of 4.2 K of both initial and treated materials and **Table 2** summarises the mechanical properties determined by the tensile tests. The initial material Mat-1 shows a tensile yield strength $\sigma_{0.2}$ of 1.17 GPa and an ultimate tensile strength σ_{max} of 1.54 GPa, whereas Mat-2 shows slightly lower values of 1.05 GPa and 1.53 GPa, respectively. The total elongation of Mat-1 exhibit 29 % and Mat-2 34 %. After deformation and annealing of the tubes, the strength increases and the strain decreases. It has been found that for Mat-1, with the slightly higher nitrogen content, higher strengths up to $\sigma_{0.2}$ = 1.35 GPa and σ_{max} = of 1.65 GPa are observed compared to Mat-2. However, for Mat-1, the achievable strain decreases down to 15 %, while Mat-2 shows still a very high elongation above 30 %. In addition, the different Nb_3Sn superconductor reaction aging treatments (HT1 and HT2) which represent different CICC preparation methods do not have such an influence.

Table 2 Average value (3 pieces for each heat treatment) of tensile properties at 4.2 K of experimental material with/without aging

Condition	$\sigma_{0.2}$ /GPa	σ_{max} /GPa	TE /%
Mat-1, as-rec.	1.17	1.54	29
Mat-1, HT1	1.35	1.65	15
Mat-1, HT2	1.28	1.61	19
Mat-2, as-rec.	1.05	1.53	34
Mat-2, HT1	1.21	1.64	30
Mat-2, HT2	1.17	1.61	35

3.2 Structural characterisation

Bragg-Brentano X-Ray diffraction pattern for as-received and treated steel samples are shown in **Fig. 2.** All samples show reflections in the XRD diagram, corresponding to the austenite phase. The splitting of the reflection originates from $K_{\alpha 1}$ and $K_{\alpha 2}$ splitting of the K_{α} doublet. Besides for Mat-2, the position in 2θ is shifted to higher angles with respect to reflections of the as-received Matl-1. After treatments broad reflections as well as a shift to similar positions in 2θ are observed.

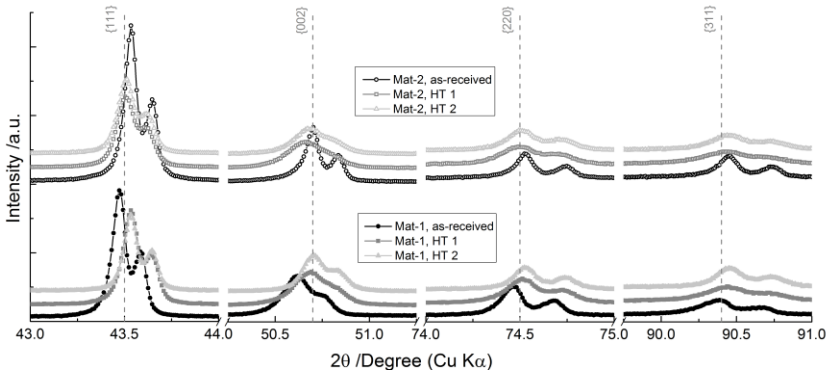

Fig. 2 Section of the XRD patterns of cross sections of the modified stainless steel with 0.174 wt.% N (Mat-1) and 0.131 wt.% N (Mat-2). Bragg positions of the standard stainless steel are indicated by dashed lines. No carbides are observed

DOI 10.12776/ams.v24i4.1140 p-ISSN 1335-1532
e-ISSN 1338-1156

After performing the cryogenic tensile tests at 4.2 K, microstructure of the deformed samples was analysed by means of BSE and EBSD. **Fig. 3** shows SEM micrographs (BSE) whereas **Fig. 4** shows the orientation mapping (colour code according to the inverse pole figure IPF of the sample surface normal) of both as-received states and both different treated samples. For both as-received states, the microstructure consists of homogenously austenite with some annealing twins. BSE images in **Fig. 3** a) and b) show, that both as-received states have no carbides or nitrides at their grain boundaries. The grain size of Mat-1 with higher nitrogen content is larger (d < 250 μm) than of Mat-2 with lower nitrogen content (d < 140 μm).

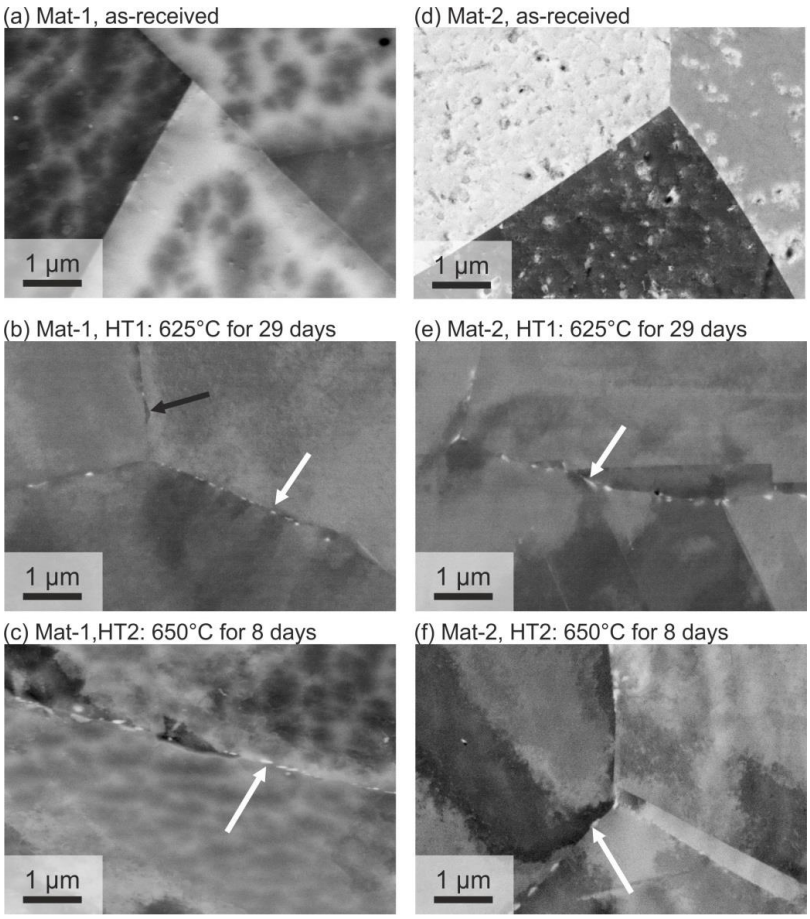

Fig. 3 Detailed SEM micrographs (BSE, orientation and composition contrast) of the modified stainless steel with 0,174 wt.% N (a-c) and with 0,131 wt.% N (d-f). For the samples after deformation and heat treatment nano carbides at grain boundaries (marked with white arrow) or nitrides (marked with black arrow) are visible

After the tube-treatment, the average size of grains does not change significantly. BSE images show precipitates at the grain boundaries. Due to the composition contrast it can be concluded that white precipitates are carbides. In addition, some dark precipitates imply that nitrides are formed. In the as-received state, twin boundaries can be identified homogenously across the cross section (white lines in **Fig. 4**). This misorientation at 60°, shown in **Fig. 5b**, is attributed to

DOI 10.12776/ams.v24i4.1140 p-ISSN 1335-1532
e-ISSN 1338-1156

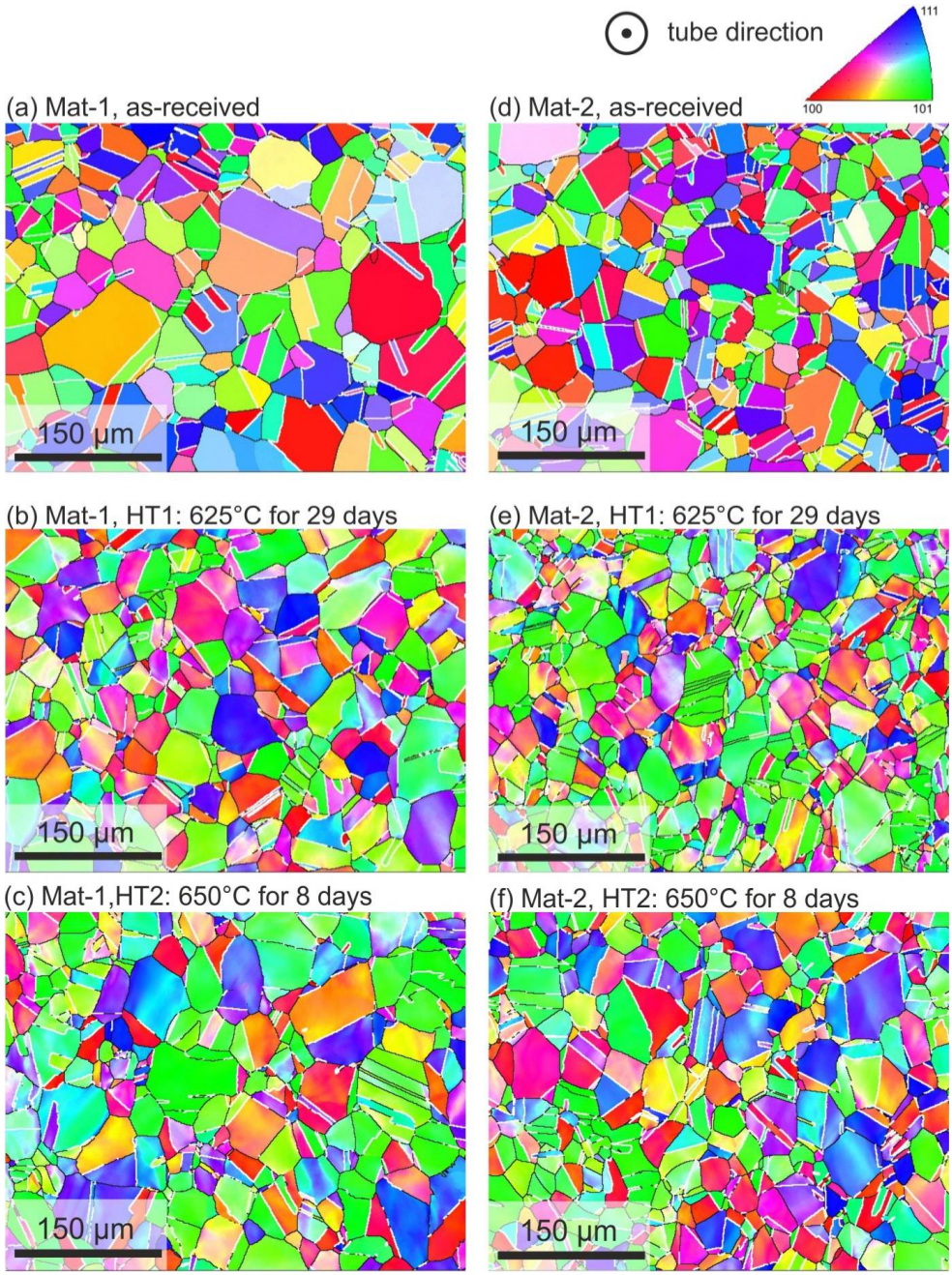

Fig. 4 Orientation image on longitudinal sections of the modified stainless steel with 0,174 wt.% N (a: as-received, b: heat treatment 1, c: heat treatment 2) - as well as with 0,131 wt.% N (d: as-received, e: heat treatment 1, f: heat treatment 2). The colour code corresponds to the inverse pole figure of the z-direction. The maps are of the same size and observed using a step size of 1 µm. White lines indicate Σ3 twin boundaries

DOI 10.12776/ams.v24i4.1140 p-ISSN 1335-1532
e-ISSN 1338-1156

Σ3 recrystallization twin boundaries of the initial microstructure. After stretching and annealing, these boundaries are changing. A lower fraction of misorientation near 60° is observed (**Fig. 5b**). The EBSD measurements (**Fig. 4**) reveal that the deformation lead to localised plastic deformation, indicated by changes of orientation contrast. The as-received state has a low average local misorientation, the maximum is close to 0.1° (**Fig. 5a**). Due to deformation the amount of larger local misorientation increases and the maximum is shifted to higher angles. For all treatments, no significant difference is visible; the maximum is at 0.4° and 0.55° for Mat-2 and HT1, respectively. From investigations of Ojima et al. [20] it is known that the nitrogen content has an influence on the local misorientation. For steels with 1 wt.% N the misorientation is higher than for low nitrogen steels (0.02 wt.%), indicating that dislocations are introduced more in high nitrogen steels than in low nitrogen steels at any given strain. In this study, the steels have a nitrogen content of 0.174 wt.% N (Mat-1) and 0.131 wt.% N (Mat-2). The difference in nitrogen is small, thus only minor changes in the misorientation distribution are expected and are confirmed by the measurements (**Fig. 5a**).

This microstructure correlate with mechanical properties as shown in **Table 2**, the yield stress of Mat-1 is larger than of Mat-2. The uniform elongation of Mat-2 is only slightly higher than of Mat-1. This is caused by work hardening.

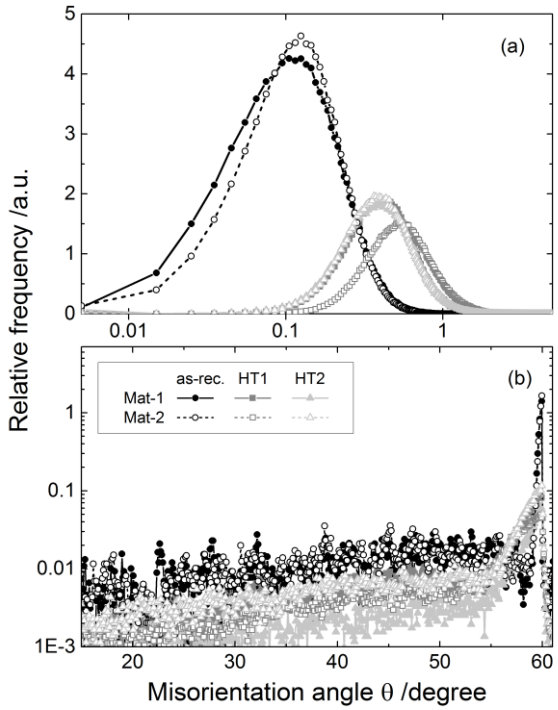

Fig. 5 Change in misorientation distribution of the modified stainless steel with 0,174 wt.% N (Mat-1, open symbols) and 0,131 wt.% N (Mat-2, closed symbols)

Conclusions

This study provides the following main results regarding microstructure and deformation at cryogenic temperature for modified stainless steels. Mechanical tensile tests of the sub-size

DOI 10.12776/ams.v24i4.1140 p-ISSN 1335-1532
e-ISSN 1338-1156

specimens at 4.2 K were performed according to ASTM standards in order to evaluate the mechanical performance after aging of stainless steels. In relation to measurements, it can be stated that:

1) Influence of heat treatment:
   - formation of fine carbides at the grain boundaries was observed, which decreases the ductility
   - aging time has no significant effect on mechanical properties and microstructure
2) Influence of nitrogen content:
   - the higher N-content the higher the austenite grain size
   - the strength (yield and uniform tensile strength) is less influenced as the elongation, which is much lower by alloying with nitrogen

These materials achieved very good results at cryogenic conditions and therefore could be possibly applied in the area of fusion.

References

[1] M. O. Hoenig, D. B. Montgomery: IEEE Transaction on Magnetics, Vol. 11, 1975, No. 4, p. 290-295
[2] T. Satow, O. Motojima: IEEE Transactions on applied superconductivity, Vol. 12, 2002, No. 1, p. 629–634
[3] J. Sapper: Superconductor Science and Technology, Vol. 13, 2000, No. 5, p. 516–518
[4] S. Ishida, P. Barabaschi, Y. Kamada: Fusion Engineering and Design, Vol. 85, 2010, No. 10-12, p. 2070–2079
[5] K. Ikeda: Nucl. Fusion, Vol. 50, 2010, No. 1, p. 1-10, DOI:10.1088/0029-5515/50/1/014002
[6] A. Devred, I. Backbier, at all: Science & Technology, Vol. 27, 2014, No. 4, p. 044001
[7] H. I. Mc Henry, R. P. Reed: Nuclear Engineering and Design, Vol. 58, 1985, No. 2, p 219-236
[8] G. Romano, A. Vostner, D. Bessette, I. Pong, G. Bevillard, C. Zhou, A. Devred: IEEE Transactions on Applied Superconductivity, Vol. 26, 2016, No. 4, DOI:10.1109%2fTASC.2016.2537919
[9] P. Czarkowski, A. T. Krawczynska, T. Brynk, M. Nowacki, M. Lewandowska, K. J. Kurzydlowski: Cryogenics, Vol. 64, 2014, p 1-4, DOI:10.1016%2fj.cryogenics.2014.07.014
[10] J. Qin, Y. Wu, K-P. Weiss, Z. Wu, L. Li: Cryogenics, Vol. 52, 2012, p. 7-9, DOI:10.1016%2fj.cryogenics.2012.02.003
[11] W. Wang, W. Yan, K. Yang, Y. Shan, Z. Jiang: Journal of Materials Engineering and Performance, Vol. 19, 2010, No. 8, p. 1214-1219, DOI:10.1007%2fs11665-010-9603-7
[12] S. T. Downey II, N. Bembridge, P. N. Kalu, H. M. Miller, G. S. Rohrer, K. Han: Journal of Materials Science, Vol. 42, 2007, No. 23, p. 9543-9547, DOI:10.1007%2fs10853-007-1959-1
[13] S. Murase, S. Kobatake, M. Tanaka, I. Tashiro, O. Horigami, H. Ogiwara, K. Shibata, K. Nagai, K. Ishikawa: Fusion Engineering and Design, Vol. 20, 1993, p. 451-454, DOI:10.1016%2f0920-3796%2893%2990078-V
[14] P. T. Purtscher, R. P. Walsh, R. P. Reed: Advances in Cryogenic Engineering, Vol. 34, 1988, p. 379-386
[15] T. Kvačkaj, R. Bidulský, A. Kováčová, J. Ileninová, J. Bidulská: Acta Metallurgica Slovaca, Vol. 20, 2014, No. 4, p. 397-404. DOI: 10.12776/ams.v20i4.438

[16] L. P. Stoter: Journal of materials science, Vol. 16, 1981, p. 1039-1051
[17] M. L. Saucedo-Muñoz, Y. Watanabe, T. Shoji, H. Takahashi: Cryogenics, Vol. 40, 2000, No. 11, p. 693-700, DOI: 10.1016/S0011-2275(01)00004-2
[18] M. Takayasu, R. A. Childs, R. N. Randall, J. V. Minervini: *IEEE Transactions on Applied Superconductivity*, Vol. 9, 1999, No. 2, p. 644–647
[19] J. Sas, K-P. Weiss, N. Bagrets: Acta Metallurgica Slovaca, Vol. 21, 2015, No. 4, p. 330-338 DOI: 10.12776/ams.v21i4.650
[20] M. Ojima, Y. Adachi, Y. Tomota, K. Ikeda, T. Kamiyama, Y. Katada: Materials Science and Engineering A, Vol. 527, 2009, p. 16–24

Acknowledgements

The author S. K.-W. gratefully acknowledge financial support by the Helmholtz Association – via the Recruitment Initiative of Prof. B. Holzapfel and the Helmholtz Energy Materials Characterization Platform (HEMCP) for funding the Bruker D8.